Structural insights into *Deinococcus radiodurans* BamA: extracellular loop diversity and its evolutionary implications

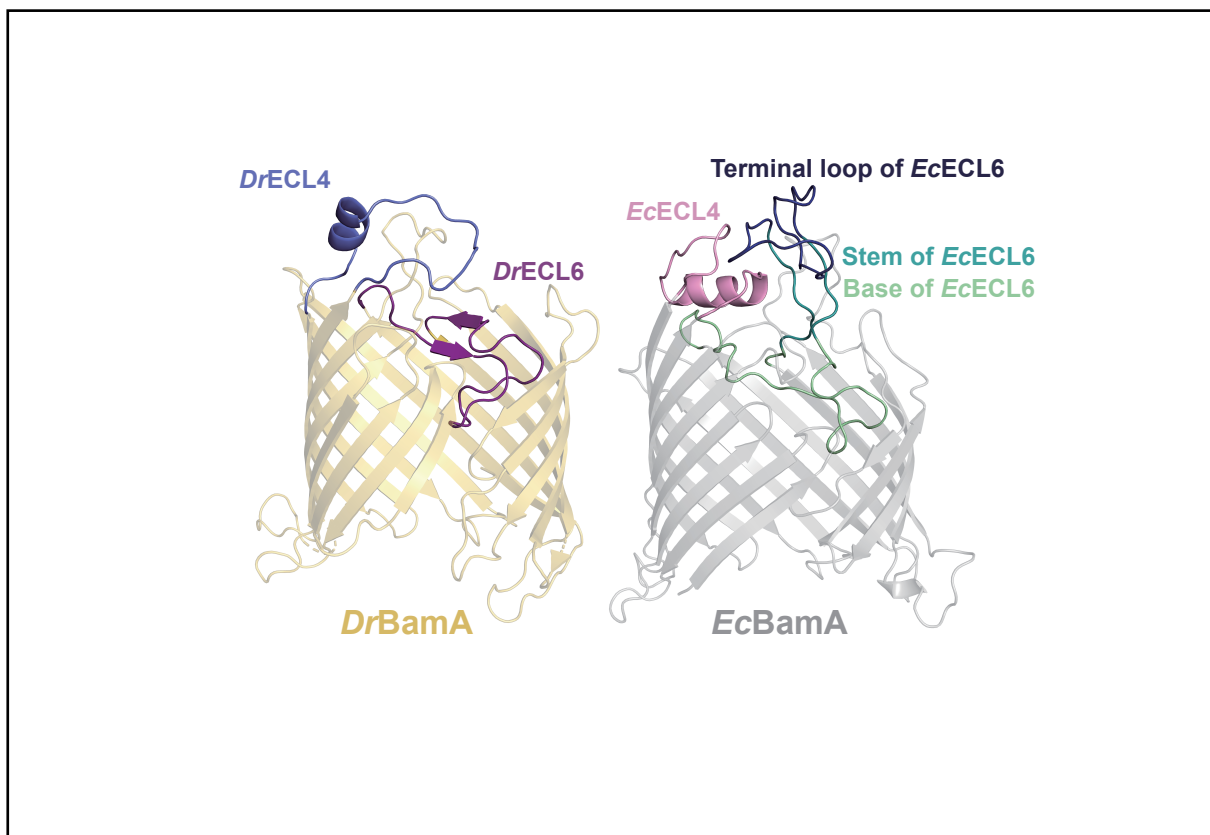Zhenzhou Wang[1], Jinchan Xue[1], Jiajia Wang[1], Jiangliu Yu[2] ✉, Hongwu Qian[1] ✉, and Xinxing Yang[1] ✉

[1]*MOE Key Laboratory for Membraneless Organelles and Cellular Dynamics, Division of Life Sciences and Medicine, University of Science and Technology of China, Hefei 230026, China;*
[2]*College of Life Science, Anhui Agricultural University, Hefei 230036, China*

✉Correspondence: Jiangliu Yu, E-mail: 2017074@ahau.edu.cn; Hongwu Qian, E-mail: hongwuqian@ustc.edu.cn; Xinxing Yang, E-mail: xinxingyang@ustc.edu.cn

Graphical abstract

Comparison of the barrel domains of DrBamA and EcBamA (PDB: 5D0O).

Public summary

■ The β-barrel domain of BamA in *Deinococcus radiodurans* and *Escherichia coli* are not interchangeable.

■ The structure of the barrel domain of *Deinococcus radiodurans* BamA reveals the difference in extracellular loop 4 and 6 compared with that in *Escherichia coli* BamA.

■ The polar interactions of the helix in extracellular loop 4 with other extracellular loops and the stem region in extracellular loop 6 are important for the function of *Escherichia coli* BamA.

Structural insights into *Deinococcus radiodurans* BamA: extracellular loop diversity and its evolutionary implications

Zhenzhou Wang[1], Jinchan Xue[1], Jiajia Wang[1], Jiangliu Yu[2] ✉, Hongwu Qian[1] ✉, and Xinxing Yang[1] ✉

[1]MOE Key Laboratory for Membraneless Organelles and Cellular Dynamics, Division of Life Sciences and Medicine, University of Science and Technology of China, Hefei 230026, China;
[2]College of Life Science, Anhui Agricultural University, Hefei 230036, China

✉Correspondence: Jiangliu Yu, E-mail: 2017074@ahau.edu.cn; Hongwu Qian, E-mail: hongwuqian@ustc.edu.cn; Xinxing Yang, E-mail: xinxingyang@ustc.edu.cn

Cite This: *JUSTC*, **2024**, 54(9): 0905 (10pp)   Read Online   SI Supporting Information

Abstract: Diderm bacteria, characterized by an additional lipid membrane layer known as the outer membrane, fold their outer membrane proteins (OMPs) via the β-barrel assembly machinery (BAM) complex. Understanding how the BAM complex, particularly its key component BamA, assists in OMP folding remains crucial in bacterial cell biology. Recent research has focused primarily on the structural and functional characteristics of BamA within the Gracilicutes clade, such as in *Escherichia coli* (*E. coli*). However, another major evolutionary branch, Terrabacteria, has received comparatively less attention. An example of a Terrabacteria is *Deinococcus radiodurans* (*D. radiodurans*), a Gram-positive bacterium that possesses a distinctive outer membrane structure. In this study, we first demonstrated that the β-barrel domains of BamA are not interchangeable between *D. radiodurans* and *E. coli*. The structure of *D. radiodurans* BamA was subsequently determined at 3.8 Å resolution using cryo-electron microscopy, revealing obviously distinct arrangements of extracellular loop 4 (ECL4) and ECL6 after structural comparison with their counterparts in gracilicutes. Despite the overall similarity in the topology of the β-barrel domain, our results indicate that certain ECLs have evolved into distinct structures between the Terrabacteria and Gracilicutes clades. While BamA and its function are generally conserved across diderm bacterial species, our findings underscore the evolutionary diversity of this core OMP folder among bacteria, offering new insights into bacterial physiology and evolutionary biology.

Keywords: BamA; extracellular loop; outer membrane protein; *Deinococcus radiodurans*

CLC number: Q932   **Document code:** A

1   Introduction

β-barrel outer membrane proteins (OMPs) are a defining feature of Gram-negative bacteria and play crucial roles in various cellular processes, including nutrient uptake, hazard shielding, and signaling. At the heart of their insertion into the outer membrane is BamA, a key component of the β-barrel Assembly Machinery (BAM) complex[1,2]. As a member of the Omp85 family, BamA is highly conserved across diderm bacteria, mitochondria, and chloroplasts[3]. In *Escherichia coli* (*E. coli*), it is one of two essential outer membrane proteins, primarily responsible for the biosynthesis of OMPs[4]. Exploring the mechanism by which BamA facilitates OMP folding is crucial for understanding membrane protein biogenesis and can provide implications for the development of antibiotics[5] that target bacterial pathogens.

Recently, significant strides have been made in elucidating the structure and function of the BAM complex, particularly in the model organism *E. coli*, primarily advanced by high-resolution cryo-electron microscopy (cryo-EM). The core protein BamA consists of two distinct regions: a C-terminal β-barrel domain, which is integrated into the outer membrane to facilitate the insertion of other OMPs, and a series of

polypeptide transport-associated (POTRA) domains located at the N-terminus[6]. These POTRA domains, which are encircled by other BAM lipoproteins (BamB-E)[7], are instrumental in directing the β-signal of unfolded OMPs to the BAM complex. The structures of several *E. coli* BAM complexes, both with and without the OMP substrate, have been resolved, allowing researchers to characterize how *Ec*BamA coordinates other BAM components and interacts with substrates to facilitate their folding and insertion process[8–12]: The periplasmic POTRA domains first recognize the C-terminal β-signal of the OMPs with the assistance of other BAM components, such as BamD. The unfolded OMP is subsequently transported to the β-barrel domain of BamA, which can open laterally and align with the substrate's last β-strand at the C-terminus. The sequential insertion of other strands of the OMP into the membrane occurs while the first strand remains coupled with BamA's β1 strand. This 'open' conformation of BamA is proposed to be a crucial intermediate state in the process of OMP folding. After complete folding and release of the OMP from the BAM complex into the hydrophobic outer membrane (OM) environment, the β1 and β16 strands of BamA reconverge into a 'closed' conformation.

Given that BamA is widely conserved, it is important to

understand whether it has a unique catalytic mechanism across various bacteria. Bioinformatic studies have shown that while most Omp85 family proteins, including BamA, share a highly similar β-barrel domain, the POTRA domains display species-specific variations in sequence and number[13,14]. These variations in the POTRA domains are thought to facilitate the recognition of different substrate proteins across various bacterial species. Additionally, the BAM accessory lipoproteins (BamB, C, D, and E in *E. coli*), which interact with one or multiple POTRA domains, have also been found to vary and are not conserved among different bacteria[7,15,16]. Replacing the POTRA domains of *Ec*BamA with those of other Gram-negative bacteria can cause cell growth defects and impede the OMP folding process[17,18]. The β-barrel domains from a range of bacteria, including *Escherichia coli*, *Pseudomonas aeruginosa* and *Neisseria meningitidis*, have been demonstrated to be functionally interchangeable[18], indicating that this domain operates via a conserved mechanism to fold OMPs, despite species differences. However, these orthologous BamA proteins predominantly originate from closely related proteobacteria species. It remains unknown whether the β-barrel domain from a distantly related bacterium could effectively replace its counterpart in *E. coli*.

Deinococcus radiodurans (*D. radiodurans* or *Dr*), a deep-branched diderm bacterium from the Deinococcota phylum (formerly Deinococcus-Thermus), which belongs to the Terrabacteria group, is thought to represent ancient evolutionary divergence[19]. Unlike its proteobacterial relatives, *D. radiodurans* possesses a distinctive outer membrane that lacks lipopolysaccharide (LPS)[20]. The BamA homolog *Dr*BamA, encoded by the DR_0379 gene, is also pivotal for cell growth, division, and stability of the cell envelope, particularly under stress conditions[21]. In contrast to *Ec*BamA from *E. coli*, which has five POTRA domains, *Dr*BamA contains six POTRA domains. Furthermore, while *E. coli* has four lipoproteins (BamB to BamE) associated with BamA, no homolog has been identified in *D. radiodurans*. These marked differences make *Dr*BamA an ideal candidate for testing the conservation of BamA's function and understanding the roles of the β-barrel domain and the POTRA domains. In this study, we determined the near-atomic resolution structure of *D. radiodurans* BamA and demonstrated that the β-barrel domains in BamA are not interchangeable between *D. radiodurans* and *E. coli*. The distinct arrangements of BamA ECL4/6 among different bacterial species highlight the evolutionary diversity of BamA and provide new insights into the evolution of diderm bacteria.

2   Materials and methods

2.1   Bacterial strains and growth conditions

DH5α[22] chemical competent cells (Alpalifebio) were used for plasmid subcloning. BL21 (DE3)[23] cells (Alpalifebio) were utilized for the expression and purification of *Dr*BamA. All other strains used for functional tests were derived from the *E. coli* BW25113 strain[24]. Lysogeny broth (LB) and agar were prepared as previously described[25]. Unless otherwise

specified, all liquid cultures were aerobically grown at 37 °C. When necessary, kanamycin (50 μg/mL), carbenicillin (50 μg/mL), streptomycin (50 μg/mL) and chloramphenicol (75 μg/mL) were added to the broth or agar. The strains are listed in Table S1 (see Supporting information).

2.2   Construction of plasmids

The dsDNA fragment encoding the signal peptide region (Met1–Ala21) and the functional region (Gln22–Trp846) of *Dr*BamA were separately amplified from the genomic DNA of *Deinococcus radiodurans* R1[26] using primers oZW1–oZW2 and oZW3–oZW4 via polymerase chain reaction (PCR), respectively (Table S1). The gene encoding the tandem Flag-tag and His$_{10}$-tag was amplified using primers oZW5 and oZW6. The gene encoding *Ec*BamA was amplified from the genomic DNA of the BW25113 strain using primers oJC38 and oJC39. Phanta Max Super-Fidelity DNA Polymerase (Vazyme, P505-d1) was employed for the PCR amplification.

pZW01–02. To express *Dr*BamA in *E. coli*, the native signal peptide (Met1–Ala21) was substituted with the 22-amino-acid pelB leader peptide from pectate lyase B in *Erwinia carotovora*, which is frequently used in the heterologous expression of outer membrane proteins in *E. coli*[27] and guides *Dr*BamA to the outer membrane. Two affinity tags (Flag-tag and His$_{10}$-tag) were inserted between pelB and *Dr*BamA (Gln22–Trp846) to generate the pelB-tag-*Dr*BamA construct (Fig. S1b). The gene encoding pelB-tag-*Dr*BamA was cloned and inserted into the pCDFDuet[28] vector. The cloning process involved two steps. First, three dsDNA fragments encoding *Dr*BamA (Met1–Ala21), Flag-His$_{10}$, and *Dr*BamA (Gln22–Trp846) were ligated and amplified via overlap PCR using primers oZW1 and oZW4. Simultaneously, the pCDFDuet vector backbone was amplified using primers oZW7 and oZW8. These two fragments were then conjugated to generate the plasmid pZW01 using the ClonExpress II One Step Cloning Kit (Vazyme, C112-01). Second, the *pelB* sequence was amplified from the pSB-13 plasmid (lab stock) using primers oZW9 and oZW10. The dsDNA encoding Flag-His$_{10}$-*Dr*BamA (Gln22–Trp846) was amplified from pZW01 using primers oZW5 and oZW8. The final plasmid, pelB-tag-*Dr*BamA (pZW02), was created by ligating these two fragments together using the ClonExpress II One Step Cloning Kit (Vazyme).

pJC06. To enable arabinose-inducible expression of wild-type *Ec*BamA, the *bamA* gene from *E. coli* was amplified and ligated with the pBAD33[29] vector backbone, which was PCR-amplified using primers oSY9 and oSY10, employing the ClonExpress II One Step Cloning Kit.

pZW23–25. To enable isopropyl β-D-thiogalactoside (IPTG)-inducible expression of *Ec*BamA and *Dr*BamA in *E. coli*, pZW24 and pZW25 were constructed on the basis of a plasmid bearing the T5lac promoter (pYD48, laboratory stock) using primers oZW29 and oZW35. For pZW24, where the wild-type *Ec*BamA was fused with a Flag-tag (for immunoblotting assays), two dsDNA fragments encoding the *Ec*BamA signal peptide (Met1–Gly20) and Flag-*Ec*BamA (Ala21–Trp810) were initially amplified from pJC06 using primers oZW31–34. These fragments were subsequently

ligated with the backbone of pYD48 using the ClonExpress II One-Step Cloning Kit. For pZW25, two dsDNA fragments encoding *Ec*BamA (Met1–Gly20) and Flag-*Dr*BamA (Gln22–Trp846) were amplified from pJC06 and pZW01 using primers oZW31–32 and oZW37–38 and ligated in the same manner. The empty vector pZW23 was constructed by amplifying and religating the backbone of the pYD48 plasmid using primers oZW29 and oZW35.

pZW26–29. Plasmids expressing chimeric *Ec*BamA variants were generated from pZW01 and pZW03. Fragments of *Dr*BamA (*Dr*B, *Dr*P, *Dr*4 and *Dr*6) were amplified from pZW01, while the fragments containing the truncated *Ec*BamA gene with the plasmid backbone were amplified from pZW23. The corresponding primers are listed in Table S1.

pZW30–34. Plasmids expressing truncated or mutated *Ec*BamA variants were generated from pZW23 through site-specific mutagenesis using Phanta Max Super-Fidelity DNA Polymerase. The primers used are listed in Table S1.

2.3 Construction of the BamA depletion strain

BW25113 wild-type *E. coli* cells were first transformed with plasmids expressing phage λ-Red recombinase (pKD46[29]) and arabinose-inducible *Ec*BamA (pJC06). The kanamycin resistance cassette (*kan* cassette) was PCR-amplified from pKD13[29] using primers oJC40 and oJC41, which flanked a 60-nt homologous sequence of the region adjacent to *bamA*. This *kan* cassette was then introduced into BW25113 cells harboring pKD46 and pJC06 to replace the native *bamA* gene via electroporation. Candidates of the BamA depletion strain were selected on LB plates supplemented with kanamycin, chloramphenicol, and 0.2% (w/v) L-arabinose and verified via colony-PCR and Sanger sequencing. The loss of the temperature-sensitive pKD46 plasmid was confirmed via colony-PCR and plating assays. The generated BamA depletion strain JC20 requires 0.2% (w/v) L-arabinose to induce BamA expression from pJC06 to support its growth. Other plasmids expressing *Ec*BamA variants were introduced into strain JC20 by electroporation and grown in the presence of 0.2% L-arabinose but without IPTG.

2.4 Protein expression and purification

E. coli BL21 (DE3) was transformed with the plasmid pZW02 to express *Dr*BamA and subsequently cultured in LB medium supplemented with streptomycin at 37 °C until the OD$_{600}$ reached 0.8. *Dr*BamA expression was induced by 0.2 mM IPTG at 37 °C for 3 h. For *Dr*BamA purification, the cells were collected and then resuspended in lysis buffer (25 mM Tris-HCl, 150 mM NaCl, pH 8.0) supplemented with 1 mM phenylmethanesulfonylfluoride (PMSF). After sonication, the cell debris was removed via centrifugation (8000 × g, 10 min, 4 °C). The supernatant was then ultracentrifuged (100000 × g, 1 h, 4 °C) to harvest the membrane pellet. The membrane pellet was then resuspended in lysis buffer, followed by the addition of 1% (w/v) lauryl maltose neopentyl glycol (LMNG) to extract membrane protein at 4 °C for 2 h. After an additional centrifugation step (23280 × g, 1 h, 4 °C), the supernatant containing solubilized membrane proteins was applied to an anti-Flag M2 affinity gel (Sigma). The resin was

washed with buffer A (25 mM Tris-HCl, 150 mM NaCl, 0.005% glyco-diosgenin (GDN), pH 8.0) and eluted with buffer A supplemented with 0.2 mg/mL Flag peptide. The eluate was further purified via size-exclusion chromatography with a Superose 6 increase 10/300 column in buffer A. The main peak fractions were collected and concentrated to approximately 4 mg/mL for cryo-EM sample preparation.

2.5 Cryo-EM sample preparation and data acquisition

To prepare the cryo-EM samples for structural analysis, 3.5 μL of purified *Dr*BamA was applied twice to glow-discharged copper grids (Quantifoil R 1.2/1.3). The grid was subsequently blotted for 3.5 s in a chamber set at 100% humidity and 8 °C and then flash-frozen in liquid ethane cooled with liquid nitrogen via a Vitrobot Mark IV (Thermo Fisher Scientific). The grid was loaded onto a Titan Krios electron microscope (FEI, Thermo Fisher Scientific) operated at 300 kV and equipped with a BioQuantum energy filter and a K3 direct electron detector (Gatan). Images were automatically acquired via EPU in superresolution mode at a nominal magnification of 81000 × g. The defocus values ranged from −1.6 to −1.8 μm. Each micrograph had an exposure time of 3.8 s, resulting in a total dose rate of approximately 50 e⁻/Å². The image stacks were motion-corrected via MotionCor2 and binned twofold, resulting in a pixel size of 1.07 Å/pixel. Moreover, dose weighting was performed[30]. Defocus values were estimated via CTFFIND4[31].

2.6 Image processing

A complete dataset comprising 4038 micrographs was collected for *Dr*BamA, from which a total of 5755354 bin2 particles were extracted via the template picker in cryoSPARC[32]. A partial dataset with 851 micrographs was selected to generate an initial 3D model. This initial model served as a reference for the selection of high-quality particles from the full dataset through Heterogeneous Refinement followed by Ab-initio Reconstructions. This process yielded a total of 728678 selected particles. These high-quality particles were employed as seeds for seed-facilitated classification[33], resulting in the identification of 1920510 good particles for the full dataset. The bin1 particles were subsequently updated. The bin1 particles selected through seed-facilitated classification underwent a single round of Heterogeneous Refinement followed by three rounds of Ab-initio Reconstruction in C1 symmetry. This led to the selection of 637638 high-quality particles and the generation of a 3D model at a resolution of 4.0 Å. These particles were further subjected to one round of Ab-initio Reconstruction in C2 symmetry, with a total of 607784 particles selected, resulting in a 3D reconstruction at 3.8 Å resolution after Non-uniform Refinement. Resolutions were estimated with the gold-standard Fourier shell correlation 0.143 criterion with high-resolution noise substitution[34,35]. The local resolution map was calculated via the "Local Resolution Estimation" tool in cryoSPARC[32].

2.7 Model building and refinement

The 3.8 Å map of *Dr*BamA was used for model building. The model was built in Coot[36], with the structure of *Dr*BamA predicted by Alphafold2[37] used as the initial model, which was

fitted into the map in ChimeraX[38]. Real-space model refinement with secondary structure and geometry restraints was conducted in PHENIX[39]. Figures showing the structure were prepared with PyMOL[40] and ChimeraX[38].

2.8　Multiple sequence alignment

The protein sequences of BamAs from different species were downloaded from the UniProt Consortium[41]. The sequences of their barrel domains were subsequently used for multiple sequence alignment via the ClustalW tool in MEGA11[42]. The phylogenetic tree in Fig. 4 was obtained from Ref. [19] and represented via iTOL v6 (https://itol.embl.de/).

2.9　Structure alignment

The structure of the barrel domain of *Dr*BamA was resolved in this study. The structures of the barrel domains of *Ec*BamA (PDB code: 5D0O)[8] and *St*BamA (PDB code: 5OR1)[46] were obtained from RSCB PDB[43,44]; the others were obtained from the AlphaFold protein structure database[45] or were predicted at a local server employing AlphaFold 2[45]. Structure alignment was conducted in PyMOL[40].

2.10　Spot assay of *Ec*BamA mutants

The BamA depletion strain, carrying different IPTG-inducible BamA variants, was initially cultured in LB media supplemented with kanamycin, chloramphenicol, carbenicillin, and 0.2% (w/v) arabinose to induce wild-type *Ec*BamA overnight at 37 °C. The overnight cultures were then diluted 1∶100 into fresh LB media supplemented with the same additives and allowed to reach the exponential growth phase at 37 °C. The cultures were subsequently further diluted to an OD_{600} of 0.5 and then subjected to a tenfold serial dilution from 10^0 to 10^{-5} in fresh LB medium. A 1 μL aliquot of each dilution was spotted onto LB plates containing 100 μM IPTG, but without arabinose, to selectively express the specific BamA variant. The plates were incubated at 37 °C for 15–20 h and photographed.

2.11　Western blot

Western blotting was performed to examine the protein expression levels of BamA variants in the membrane. Five hundred milliliters of JC20 cells transformed with BamA variants were cultured to the exponential growth phase as described in Section 2.10. The BamA variants were subsequently induced with 0.1 mM IPTG for 1.5 h at 37 °C. Then, the cells were collected and resuspended in approximately 25 mL of lysis buffer and sonicated. The cell debris and unbroken cells were removed by centrifugation at 8000 × g for 10 min. The supernatant was centrifuged at 100000 × g for 60 min, and the membrane pellet was collected. The membrane pellet was suspended in lysis buffer and then solubilized with LMNG for 1 h at 4 °C. After centrifugation (23800 × g, 1 h, 4 °C), the supernatant was normalized by the Bradford (Bio-red) to a total concentration of protein at 4 mg/mL. The samples were mixed with 5×SDS–PAGE loading buffer and then heated for 20 min at 95 °C. The samples were subjected to SDS–PAGE and transferred to PVDF membranes. The PVDF membranes were blocked with nonfat milk (5%) for 1 h at room temperature and then incubated with anti-Flag (for BamA variants) and anti-FtsI (for FtsI) antibodies. The PVDF membranes were washed with TBST 3 times and then incubated with the corresponding secondary antibodies. The PVDF membranes were washed with TBST 3 times and then detected.

3　Results

3.1　The β-barrel domain of BamA is not always interchangeable

To increase our understanding of the function of BamA across different bacterial species, we compared the structural intricacies of *Ec*BamA[8] with those of five proteobacterial BamAs, referencing data from the RCSB PDB[43,44] and the AlphaFold Database[45]. The analysis, which focused on β-barrel domains, revealed striking similarities, with minimal divergence in the root mean square deviation (RMSD) values, which were all less than 1.1 Å (Fig. 1a). Multiple sequence alignment (MSA) revealed lower sequence similarity of *Dr*BamA's barrel domain to that of proteobacteria BamAs (Fig. 1b, Fig. S1a), suggesting relatively large differences between their barrel domains. Interestingly, the extracellular loops of *Dr*BamA are particularly different.

We first created an *E. coli* BamA depletion strain (JC20), with the native *bamA* gene replaced by a kanamycin resistance cassette and complemented with wild-type *Ec*BamA on an L-arabinose-inducible plasmid (pJC06) (Fig. 1c). We then introduced *Dr*BamA, or its specific domains, via a separate IPTG-inducible plasmid (Fig. 1c). The results of the spot assay revealed that full-length *Dr*BamA expression was lethal, even worse than that of the empty vector (EV) control (Fig. 1d, lines 1–3), suggesting some type of dominant negative effect of the heterogeneity of *Dr*BamA in *E. coli*. Since the lipoprotein components and the number of BamA POTRA domains in *D. radiodurans* are different from those in *E. coli*, this difference is likely due to the inability of *Dr*BamA POTRA domains to recognize the β-signals of *E. coli* OMPs. This finding aligns with previous studies on full-length BamA replacements[17]. The minimum growth of the empty vector control (10^0 dilution) is likely attributable to the basal level expression of wild-type BamA from the pBAD vector. Accordingly, replacing the POTRA domains of *Ec*BamA (Ala21–Thr423) with *Dr*BamA (Gln22–Gly480, *Dr*P) also caused severe cell death, similar to full-length replacement (Fig. 1d, line 4). Furthermore, we explored the interchangeability of the β-barrel domains between *Ec*BamA and *Dr*BamA by substituting the β-barrel domains of *Ec*BamA (Gly424–Trp810) with those of *Dr*BamA (Ile481–Trp846, referred to as *Dr*B). Interestingly, *E. coli* cells expressing *Ec*BamA (*Dr*B) also presented severe growth deficiency in terms of cell growth (Fig. 1d, line 5), indicating that the β-barrel domain is not universally interchangeable, especially when the sequence similarity diverges significantly (Fig. S1a). The western blot results confirmed that *Dr*BamA and the chimeric *Ec*BamAs were expressed and folded in *E. coli* (Fig. S3a), suggesting that these proteins are dysfunctional in facilitating the folding of other OMPs in this bacterium.
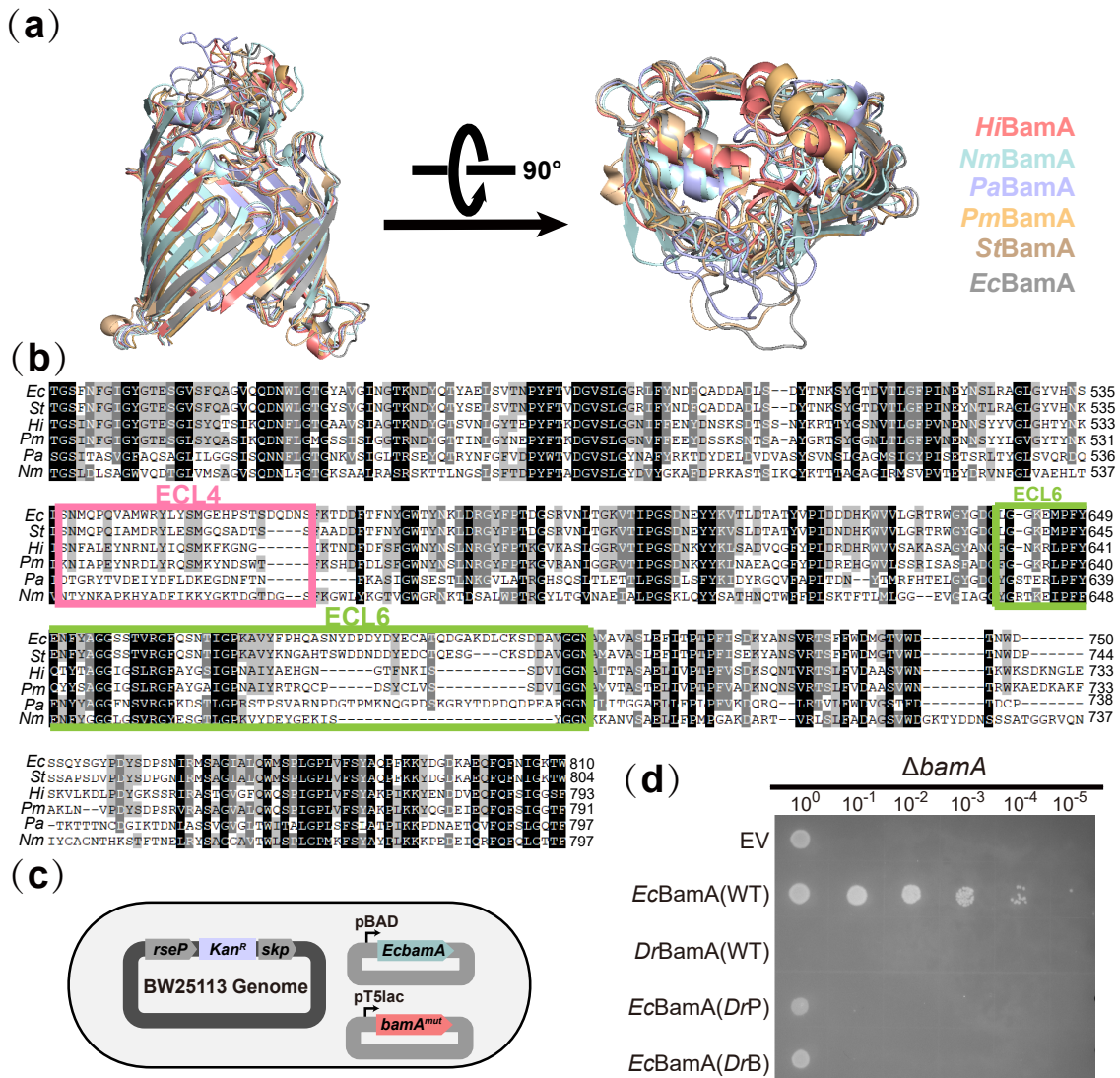
Fig. 1. Chimeric *Ec*BamA carrying the β-barrel domain of *Dr*BamA cannot rescue the loss of native *Ec*BamA. (a) Comparison of the barrel domain of BamA orthologs from several gamma- and beta-proteobacteria. *Ec*: *E. coli, St*: *Salmonella enterica serovar Typhimurium, Hi*: *Haemophilus influenzae, Pm*: *Pasteurella multocida, Pa*: *Pseudomonas aeruginosa, Nm*: *Neisseria meningitidis*. The structures of the barrel domains of *Ec*BamA (PDB code: 5D0O)[8] and *St*BamA (PDB code: 5OR1)[46] were obtained from RSCB PDB[43, 44], and the others were obtained from the AlphaFold Protein Structure Database[45]. (b) Sequence alignment of the barrel domain of BamA orthologs from the species in (a). ECL4 and ECL6 of *Ec*BamA were labeled. (c) Schematic diagram of the BamA depletion strain. (d) Spot assay of full-length *Dr*BamA and the chimera BamA carrying different domains of *Dr*BamA and *Ec*BamA. EV: empty vector. The results are representative of at least three independent experiments. The same applies hereinafter.

3.2 Structural insights into the *Dr*BamA β-barrel domain through cryo-EM analysis

To further investigate why the *Ec*BamA (*Dr*B) chimera fails to function in *E. coli* cells, unlike other proteobacterial BamA orthologs, we embarked on a detailed structural analysis of the *Dr*BamA β-barrel domain (Fig. 2a) via cryo-EM single-particle analysis. We first modified the signal peptide of *Dr*BamA to pelB to ensure heterogeneous expression and proper folding within the *E. coli* outer membrane (Fig. S1b). After detergent screening, *Dr*BamA was extracted with LMNG and purified in the presence of GDN micelles, resulting in well-behaved proteins. Then, cryo-EM samples were prepared, and a dataset with 4038 movies was collected for structural determination (Fig. S1c). The initial 2D classification revealed that *Dr*BamA predominantly exists in a dimeric

form (Fig. S1d). Finally, the cryo-EM map of *Dr*BamA was determined at 3.8 Å resolution using 607784 selected particles with C2 symmetry, revealing the intricacies of the barrel domain (Fig. 2b–c, Fig. S1e, and Table S2). Notably, all six POTRA domains were absent from the structure, implying their inherent flexibility —this aligns with findings from previous studies, such as that on *Salmonella enterica serovar Typhimurium* BamA[46].

A detailed dimeric model was constructed on the basis of the 3.8 Å cryo-EM map, of which 369 side chains (Arg478–Trp846) were assigned to each protomer (Fig. S1, Fig. S2). Each protomer has a classic 16 transmembrane β-strands architecture with prominent extracellular loops, such as ECL4 and ECL6. The size and shape of the barrel are comparable to those of *Ec*BamA (40 Å in length, 24 Å in width, and 32 Å in height, Fig. 2c–e)[8]. Moreover, both protomers
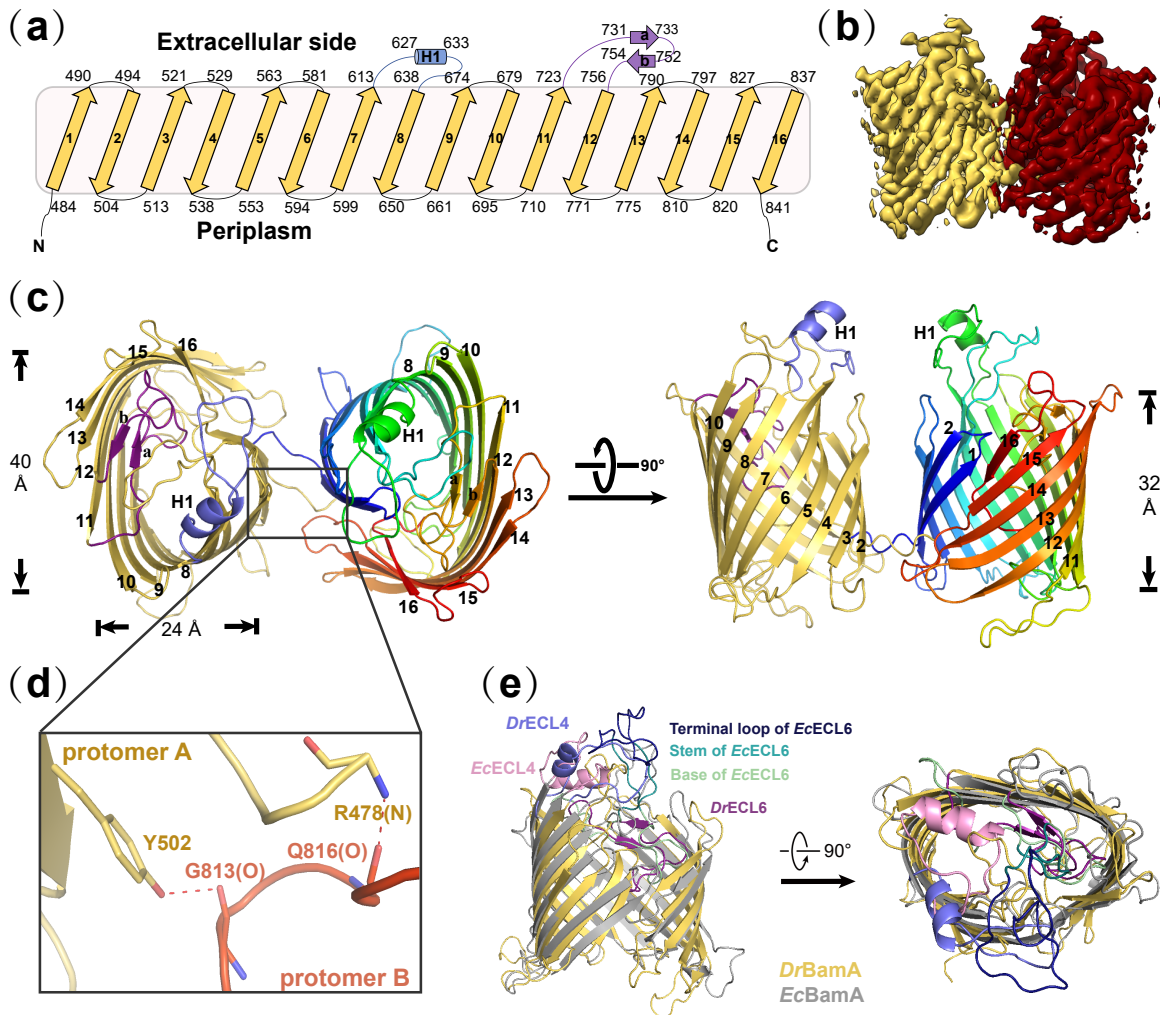
Fig. 2. Overall structure of the *Dr*BamA dimer. (a) Topologic model of the *Dr*BamA barrel domain. β-strands are shown as arrows, and the α-helix is shown as a cylinder. The transmembrane sheets, ECL4 and ECL6, are colored yellow orange, slate and deep purple, respectively. (b) Cryo-EM map of dimeric *Dr*BamA with each protomer in individual colors. (c) Cartoon representation of the *Dr*BamA dimer from the side view and top view, with one protomer colored rainbow and the other colored as in (a). (d) Polar interactions between the two protomers of *Dr*BamA. (e) Comparison of the barrel domains of *Dr*BamA and *Ec*BamA (PDB: 5D0O)[8].

were observed in the 'closed' conformation[8]. Two polar interactions between the two protomers, Arg478–Gln816 and Tyr502–Gly813, were observed in the structure (Fig. 2d).

Furthermore, the significant increase in the root mean square deviation (RMSD) to 2.5 Å compared with that of *Ec*BamA (PDB: 5D0O)[8] underscores a distinct structural divergence, especially in the altered shape, position, and orientation of ECL4 and ECL6 (Fig. 2e). These structural discrepancies may contribute to the functional deficiencies observed in the *Ec*BamA (*Dr*B) chimera.

3.3 The structural and functional roles of ECL4 and ECL6 in *Ec*BamA and *Dr*BamA

To determine whether variations in the ECL4 and ECL6 structures of BamA affect its function, we meticulously compared these extracellular loops between *Dr*BamA and proteobacterial BamAs. All the BamAs exhibit an α-helix with 7–12 residues (hereafter the outer helix) within ECL4 (Fig. 3a), albeit with *Dr*BamA's helix being more peripherally positioned and tilted (Fig. 2e). Conversely, the ECL6 of

proteobacterial BamA presents a 'hairpin-like' topology comprising a 'base', a 'stem', and a 'terminal loop', whereas *Dr*BamA's ECL6 is notably different, lacking the stem and terminal loop (Fig. 3b). In both 'closed'[8] and 'open'[11] conformations, the ECL6 of *Ec*BamA consistently adopts a 'hairpin' topology that protrudes toward the extracellular side (Fig. 2e and Fig. 3d).

Intrigued by these structural variances, we hypothesized that substituting ECL4 or ECL6 of *Ec*BamA with those from *Dr*BamA might shed light on their roles in OMP folding. Initially, we engineered chimeric versions of *Ec*BamA by replacing its entire ECL4 (Asn538–Asn563) and ECL6 (Leu641–Asn709) with the corresponding sequences from *Dr*BamA (ECL4: Leu614–Thr637; ECL6: Asp727–Thr755), resulting in *Ec*BamA (*Dr*4) and *Ec*BamA (*Dr*6), respectively. Furthermore, we combined both modifications to create a double substitution variant, *Ec*BamA (*Dr*4+*Dr*6). Western blot analysis revealed that these chimeric *Ec*BamAs were expressed at levels similar to the WT *Ec*BamA in *E. coli* (Fig. S3b). Spot assays revealed that *Ec*BamA (*Dr*4+*Dr*6) signific-
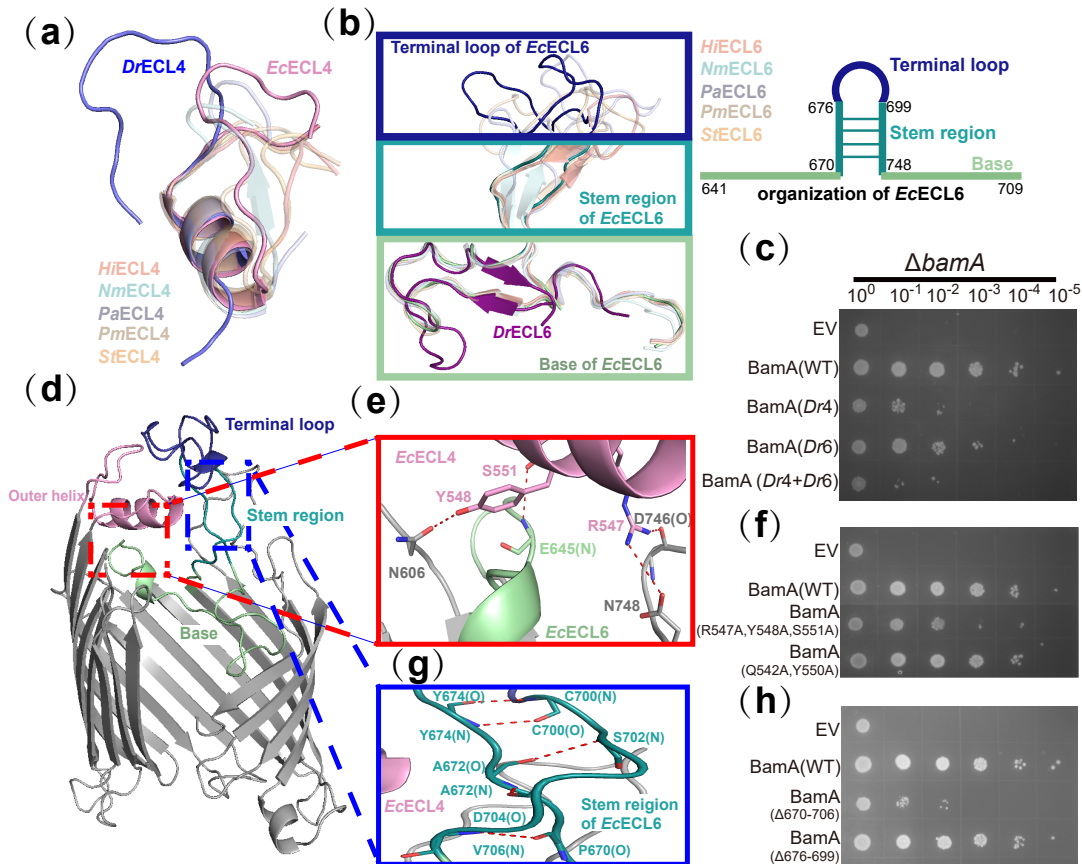
Fig. 3. Analysis of ECL4 and ECL6 in BamA. (a, b) Structural alignments of ECL4s (a) and ECL6s (b) in BamA orthologs from different species. The ECL4 and ECL6 products from the proteobacteria were obtained and colored the same as those in Fig. 1(a). The "hairpin-like" topological organization of *Ec*ECL6 is shown in addition to the comparison of the ECL6s. (c) Spot assays in which the chimera *Ec*BamA replaced ECL4 or ECL6 with the corresponding region of *Dr*BamA. (d) Overall structure of the *Ec*BamA barrel domain in the intermediate-open state (PDB: 7TT6) [11]. (e) Polar interactions between residues in the outer helix with other extracellular loops in *Ec*BamA. (f) Spot assays of mutants in the outer helix of *Ec*BamA. (g) Hydrogen bonds of the residues in the stem region of *Ec*ECL6. (h) Spot assays of different truncated versions of ECL6 in *Ec*BamA. Each region was deleted by replacement with a GS linker (GSGS for "del 670–706" and GSG for "del 676–699").

antly impeded cell growth, mirroring the effect observed with the empty vector control (Fig. 3c, line 5). Substitution of either loop individually also led to a remarkable decrease in cell viability by 1–2 orders of magnitude (Fig. 3c, lines 3–4), with ECL4 replacement being more detrimental than ECL6. These results support our hypothesis that extracellular loops are essential for the folding process.

To understand the specific functional impacts of the distinct regions of ECL4 and ECL6, we determined that in *Ec*BamA, the outer helix of ECL4 is characterized by three polar residues (Arg547, Tyr548, and Ser551) forming polar interactions with adjacent loops (ECL7, ECL5, and ECL6) in its open conformation[11] (Fig. 3d, e). In contrast, the outer helix of *Dr*BamA predominantly comprises hydrophobic residues and lacks polar interactions with adjacent loops, which may contribute to its tilted orientation (Fig. 2e) and functional discrepancies. The impaired functionality of *Ec*BamA (*Dr*4) underscores the potential role of these polar residues in the OMP folding mechanism in *E. coli*. To further ascertain the significance of these polar residues, we substituted them with hydrophobic alanine (R547A, Y548A, S551A). The mutation significantly compromised the function of *Ec*BamA (Fig. 3f, line 3). Conversely, the function of *Ec*BamA remained relatively stable when adjacent polar

residues were mutated to alanine (Q542A, Y550A) (Fig. 3f, line 4). Given that the expression levels of the mutated *Ec*BamA were not significantly affected (Fig. S3c), the results suggest critical roles for specific polar interactions between the outer helix and adjacent ECLs for BamA functionality in *E. coli*. This conclusion is supported by the lethal effect of mutating Arg547 to alanine observed in a previous study[47]. However, in the distantly related ancient diderm bacterium *D. radiodurans*, such interactions appear nonessential, suggesting a different, yet to be elucidated, mechanism by which ECL4 contributes to the OMP folding process.

With respect to ECL6, all the BamA orthologs investigated in this study feature a similarly structured 'base' (Fig. 3b). Proteobacterial BamAs, however, possess an additional loop structure (Pro670–Val706 in *Ec*BamA), albeit these are less conserved according to multiple sequence alignment (MSA) (Fig. 1b). Structurally, the loop is composed of a 'stem' region stabilized with hydrogen bonds and an elongated 'terminal loop' connected in between (Fig. 3b and g). To probe the functional importance of different regions of this loop, we engineered various *Ec*BamA truncations, which can be expressed normally in *E. coli* (Fig. S3d), for spot assays. Notably, removing only the terminal loop residues (Pro676–Leu699) did not significantly affect the functional-

ity of *Ec*BamA (Fig. 3b and h, line 4). However, deleting both the stem and terminal loop (residues 670–706) resulted in severe functional loss, nearly equivalent to the empty vector control (Fig. 3h, line 3). This deficiency was even more pronounced than that of *Ec*BamA, with the entire ECL6 replaced by *Dr*BamA (Fig. 3c, line 4), emphasizing the critical role of the stem region (Pro670–Phe675, Cys700–Val706) in stabilizing ECL6 or assisting in OMP folding in proteobacteria. This finding is consistent with previous findings in which deleting residues 673–702 of BamA was shown to be lethal in *E. coli*[48]. Intriguingly, *Dr*BamA's base region contains antiparallel sheets, potentially offering similar ECL6 stabilization functions.

The results of the spot assay combined with the structural comparison demonstrated that ECL4 and ECL6 are critical for the functionality of BamA, particularly the role of the outer helix of ECL4 and the stem region of ECL6 in the folding process of *Ec*BamA and likely other proteobacterial BamAs.

4 Discussion

In diderm bacteria, the outer membrane is replete with β-barrel proteins (OMPs). Central to assisting their folding is the BAM complex, with BamA serving as the core component. Recent advances, particularly in cryo-EM, have shed light on the mechanism of BamA in facilitating the folding of other OMPs and itself[8–12]. The working model is that POTRA domains (and other BAM components) guide OMP C-terminal β-signals to the β-barrel of BamA, which facilitates folding and insertion into the hydrophobic lipid layer.

D. radiodurans is part of the Deinococcota phylum, which belongs to the larger Terrabacteria clade, alongside other phyla such as Cyanobacteriota, Bacillota, Actinomycetota, Synergistota, Thermotogota, and Chloroflexota. This group includes both diderm and monoderm bacteria, whereas the Gracilicutes clade comprises exclusively diderm bacterial phyla, including Pseudomonadota, the Planctomycetes/Verrucomicrobia/Chlamydiae superphylum, Bacteroidota, and Spirochaetota (Fig. 4)[49]. Recent studies have suggested that these groups diverged following an ancient event characterized by distinct outer membrane tethering systems to the peptidoglycan cell wall[19]. *Dr*BamA and *Ec*BamA exhibit considerable differences: *Ec*BamA features five POTRA domains and four assessor lipoproteins (BamB-E), whereas *Dr*BamA contains six POTRA domains but lacks any identified lipoprotein partners. We propose that an in-depth analysis of BamA structure and function in *E. coli* and *D. radiodurans* could offer novel insights into the evolutionary development of bacterial outer membranes. On the basis of the aforementioned differences, it is not surprising that the POTRA domain of *Ec*BamA cannot be replaced with the corresponding region of *Dr*BamA. Some studies have indicated that the β-barrel domain of various proteobacterial BamAs is interchangeable[18], reflecting a possibly conserved folding mechanism. However, our results revealed that the barrel domain of *Ec*BamA cannot be substituted with that of *Dr*BamA, indicating differences between their barrel domains.

To examine the structural differences, we resolved *Dr*BamA's structure through cryo-EM at a resolution of 3.8
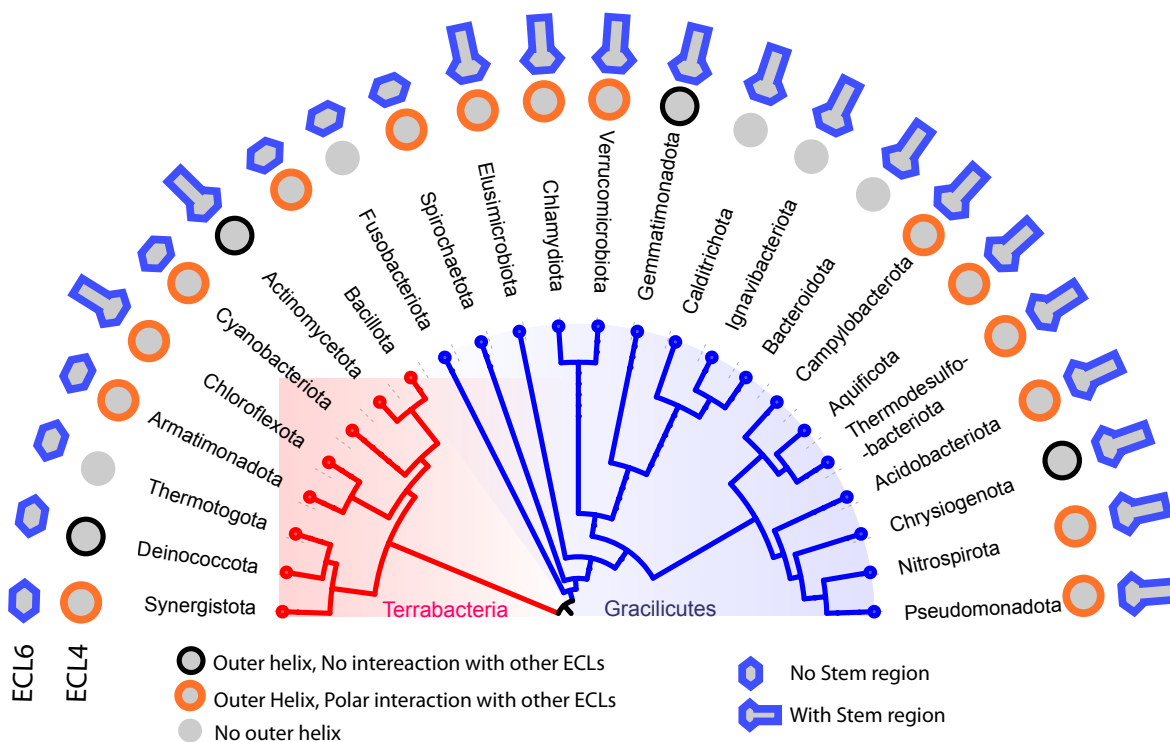

Fig. 4. Mapping of ECL4 and ECL6 features on bacterial phylogeny. This figure presents a phylogenetic tree based on Witwinowski et al.[19], collapsed at the phylum level via iTOL v6 (https://itol.embl.de/). It includes one or two BamA structures from each phylum, sourced from previous studies, this research, or AlphaFold2[45] predictions. ECL4 is categorized as either possessing an outer helix or not, with those containing an outer helix further classified on the basis of polar interactions with other extracellular loops. ECL6 classification hinges on the presence of a stem region. The detailed species names and corresponding UniProt accession numbers are available in Table S3.

Å, finding that its barrel domain is broadly similar to the 16-strand β-barrel topology of *Ec*BamA but has distinctly arranged extracellular loops, such as ECL4 and ECL6. Substituting these critical loops in *Ec*BamA with those from *Dr*BamA resulted in significant functional impairment, emphasizing their importance in BamA's function. Specifically, the ECL4 of *Ec*BamA contains a short helix with three polar residues that form key polar interactions with adjacent loops, a feature that is conspicuously absent in *Dr*BamA. Our spot assays confirmed the importance of these interactions in *E. coli*, alongside the essentiality of the stem region in ECL6, which was also absent in *Dr*BamA.

To further explore the potential connections in outer membrane evolution, we analyzed 24 BamA proteins from eight diderm phyla in Terrabacteria and sixteen from phyla in Gracilicutes, following the categorization by Witwinoski et al.[19] (Fig. 4, Table S3). The structures of these BamAs were either resolved in this study (like *Dr*BamA), obtained from previous studies (such as *Ec*BamA[8], *St*BamA[46], and *Ng*BamA[48]) or predicted via AlphaFold2[45] (Fig. 3 and Fig. S4). While no clear pattern was evident in the ECL4 loop across the two bacterial clades, our analysis revealed a notable difference in the ECL6 loop. Specifically, 14 of the 16 BamAs examined in Gracilicutes bacteria presented a stem region in their ECL6 loop. In contrast, this feature was found in only two of the eight BamAs from the Terrabacteria clade, as shown in Fig. 4. This distinct structural variation in the ECL6 loop highlights differences between these major bacterial clades in the core OMP folding protein BamA. We speculate that variations in lipids in the outer membrane among species may serve as selection pressures in the evolution of BamA, potentially contributing to the observed structural deviations in ECL6 across different bacterial clades. For example, a notable characteristic of the outer membrane of *D. radiodurans* is its absence of LPS in the outer leaflet[20], which imparts asymmetry to the outer membrane and influences its fluidity and charge.

Unfortunately, it is unclear whether *Dr*BamA tends to form intrinsic dimers or if the dimeric structure reflects the last stage of BamA folding. More experiments are needed to determine whether *Dr*BamA forms a functional dimer in the native state.

5 Conclusions

Overall, this study elucidates the crucial roles of BamA's β-barrel and extracellular loops in OMP folding, revealing significant structural and functional divergences across bacteria. The inability to interchange domains between *Ec*BamA and the evolutionarily distinct *Dr*BamA, alongside the critical importance of specific loop interactions, underscores the evolutionary complexity and specificity of the mechanisms of OMP folding. This research emphasizes the need to broaden our understanding of outer membrane protein folding mechanisms in various microbial organisms, which could unveil novel insights into bacterial physiology and evolution.

Supporting information

The supporting information for this article can be found online at https:// doi.org/10.52396/JUSTC-2024-0012. The supporting information includes four figures and three tables.

Conflict of interest

The authors declare that they have no conflict of interest.

Biographies

Zhenzhou Wang is a graduate student at the Division of Life Science and Medicine, University of Science and Technology of China, under the supervision of Prof. Hongwu Qian. His research mainly focuses on the structure and function of important membrane proteins in bacteria.

Jiangliu Yu is currently a Lecturer at Anhui Agricultural University. He received his Ph.D. degree from Zhejiang University under the tutelage of Prof. Bing Tian and Prof. Yuejin Hua in 2017. His research interests include environmental stress resistance of bacteria and bacterial cell structure.

Hongwu Qian is currently a Professor of the Division of Life Science and Medicine, University of Science and Technology of China. He received his B.S. degree from Huazhong University of Science and Technology in 2013 and Ph.D. degree from Tsinghua University in 2018. His research interests include the molecular basis of essential membrane proteins.

Xinxing Yang is currently a Professor of the Division of Life Science and Medicine, University of Science and Technology of China. He received his B.S. degree from Peking University in 2006 and Ph.D. degree from Peking University in 2012. His research interests include the biophysics and cell biology of bacteria.

References

[1] Tomasek D, Kahne D. The assembly of β-barrel outer membrane proteins. *Current Opinion in Microbiology*, **2021**, *60*: 16–23.

[2] Wu R, Stephenson R, Gichaba A, et al. The big BAM theory: An open and closed case. *Biochimica et Biophysica Acta (BBA) - Biomembranes, 2020*, **1862** (1): 183062.

[3] Webb C T, Heinz E, Lithgow T. Evolution of the β-barrel assembly machinery. *Trends in Microbiology*, **2012**, *20* (12): 612–620.

[4] Horne J E, Brockwell D J, Radford S E. Role of the lipid bilayer in outer membrane protein folding in Gram-negative bacteria. *The Journal of Biological Chemistry*, **2020**, *295* (30): 10340–10367.

[5] Kaur H, Jakob R P, Marzinek J K, et al. The antibiotic darobactin mimics a β-strand to inhibit outer membrane insertase. *Nature*, **2021**, *593*: 125–129.

JUSTC
Structural insights into *Deinococcus radiodurans* BamA: extracellular loop diversity and its evolutionary implications
Wang et al.

[6] Noinaj N, Gumbart J C, Buchanan S K. The β-barrel assembly machinery in motion. *Nature Reviews Microbiology*, **2017**, *15*: 197–204.

[7] Anwari K, Webb C T, Poggio S, et al. The evolution of new lipoprotein subunits of the bacterial outer membrane BAM complex. *Molecular Microbiology*, **2012**, *84* (5): 832–844.

[8] Gu Y, Li H, Dong H, et al. Structural basis of outer membrane protein insertion by the BAM complex. *Nature*, **2016**, *531*: 64–69.

[9] Tomasek D, Rawson S, Lee J, et al. Structure of a nascent membrane protein as it folds on the BAM complex. *Nature*, **2020**, *583*: 473–478.

[10] Wu R, Bakelar J W, Lundquist K, et al. Plasticity within the barrel domain of BamA mediates a hybrid-barrel mechanism by BAM. *Nature Communications*, **2021**, *12*: 7131.

[11] Doyle M T, Jimah J R, Dowdy T, et al. Cryo-EM structures reveal multiple stages of bacterial outer membrane protein folding. *Cell*, **2022**, *185* (7): 1143–1156.

[12] Shen C R, Chang S H, Luo Q H, et al. Structural basis of BAM-mediated outer membrane beta-barrel protein assembly. *Nature*, **2023**, *617*: 185–193.

[13] Arnold T, Zeth K, Linke D. Omp85 from the thermophilic cyanobacterium *Thermosynechococcus elongatus* differs from proteobacterial Omp85 in structure and domain composition. *The Journal of Biological Chemistry*, **2010**, *285* (23): 18003–18015.

[14] Koenig P, Mirus O, Haarmann R, et al. Conserved properties of polypeptide transport-associated (POTRA) domains derived from cyanobacterial Omp85. *Journal of Biological Chemistry*, **2010**, *285* (23): 18016–18024.

[15] Gatsos X, Perry A J, Anwari K, et al. Protein secretion and outer membrane assembly in *Alphaproteobacteria*. *FEMS Microbiology Reviews*, **2008**, *32* (6): 995–1009.

[16] Estrada Mallarino L, Fan E, Odermatt M, et al. TtOmp85, a β-barrel assembly protein, functions by barrel augmentation. *Biochemistry*, **2015**, *54* (3): 844–852.

[17] Volokhina E B, Grijpstra J, Beckers F, et al. Species-specificity of the BamA component of the bacterial outer membrane protein-assembly machinery. *PLoS One*, **2013**, *8* (12): e85799.

[18] Browning D F, Bavro V N, Mason J L, et al. Cross-species chimeras reveal BamA POTRA and β-barrel domains must be fine-tuned for efficient OMP insertion. *Molecular Microbiology*, **2015**, *97* (4): 646–659.

[19] Witwinowski J, Sartori-Rupp A, Taib N, et al. An ancient divide in outer membrane tethering systems in bacteria suggests a mechanism for the diderm-to-monoderm transition. *Nature Microbiology*, **2022**, *7* (3): 411–422.

[20] Sexton D L, Burgold S, Schertel A, et al. Super-resolution confocal cryo-CLEM with cryo-FIB milling for *in situ* imaging of *Deinococcus radiodurans*. *Current Research in Structural Biology*, **2022**, *4*: 1–9.

[21] Yu J L, Lu L C. BamA is a pivotal protein in cell envelope synthesis and cell division in *Deinococcus radiodurans*. *Biochimica et Biophysica Acta (BBA) - Biomembranes*, **2019**, *1861* (7): 1365–1374.

[22] Chen J C, Li Y, Zhang K, et al. Whole-genome sequence of phage-resistant strain *Escherichia coli* DH5α. *Genome Announcements*, **2018**, *6* (10): e00097–18.

[23] Wood W B. Host specificity of DNA produced by *Escherichia coli*: Bacterial mutations affecting the restriction and modification of DNA. *Journal of Molecular Biology*, **1966**, *16* (1): 118–133.

[24] Baba T, Ara T, Hasegawa M, et al. Construction of *Escherichia coli* K-12 in-frame, single-gene knockout mutants: the Keio collection. *Molecular Systems Biology*, **2006**, *2*: 2006.0008.

[25] Silhavy T J, Berman M L, Enquist L W. Experiments With Gene Fusions. Cold Spring Harbor, NY: Cold Spring Harbor Laboratory, **1984**.

[26] White O, Eisen J A, Heidelberg J F, et al. Genome sequence of the radioresistant bacterium *Deinococcus radiodurans* R1. *Science*, **1999**, *286* (5444): 1571–1577.

[27] Anand A, LeDoyt M, Karanian C, et al. Bipartite topology of *Treponema pallidum* repeat proteins C/D and I: outer membrane insertion, trimerization, and porin function require a C-terminal β-barrel domain. *The Journal of Biological Chemistry*, **2015**, *290* (19): 12313–12331.

[28] Walters K A, Golbeck J H. Expression, purification and characterization of an active C491G variant of ferredoxin sulfite reductase from *Synechococcus elongatus* PCC 7942. *Biochimica et Biophysica Acta (BBA) - Bioenergetics*, **2018**, *1859* (10): 1096–1107.

[29] Datsenko K A, Wanner B L. One-step inactivation of chromosomal genes in *Escherichia coli* K-12 using PCR products. *Proceedings of the National Academy of Sciences of the United States of America*, **2000**, *97* (12): 6640–6645.

[30] Grant T, Grigorieff N. Measuring the optimal exposure for single particle cryo-EM using a 2.6 Å reconstruction of rotavirus VP6. *eLife*, **2015**, *4*: e06980.

[31] Rohou A, Grigorieff N. CTFFIND4: Fast and accurate defocus estimation from electron micrographs. *Journal of Structural Biology*, **2015**, *192* (2): 216–221.

[32] Punjani A, Rubinstein J L, Fleet D J, et al. cryoSPARC: algorithms for rapid unsupervised cryo-EM structure determination. *Nature Methods*, **2017**, *14*: 290–296.

[33] Wang N, Jiang X, Zhang S, et al. Structural basis of human monocarboxylate transporter 1 inhibition by anti-cancer drug candidates. *Cell*, **2021**, *184* (2): 370–383.

[34] Chen S, Mcmullan G, Faruqi A R, et al. High-resolution noise substitution to measure overfitting and validate resolution in 3D structure determination by single particle electron cryomicroscopy. *Ultramicroscopy*, **2013**, *135*: 24–35.

[35] Rosenthal P B, Henderson R. Optimal determination of particle orientation, absolute hand, and contrast loss in single-particle electron cryomicroscopy. *Journal of Molecular Biology*, **2003**, *333* (4): 721–745.

[36] Emsley P, Lohkamp B, Scott W G, et al. Features and development of *Coot*. *Acta Crystallographica Section D: Structural Biology*, **2010**, *66*: 486–501.

[37] Tunyasuvunakool K, Adler J, Wu Z, et al. Highly accurate protein structure prediction for the human proteome. *Nature*, **2021**, *596*: 590–596.

[38] Goddard T D, Huang C C, Meng E C, et al. UCSF ChimeraX: Meeting modern challenges in visualization and analysis. *Protein Science*, **2018**, *27* (1): 14–25.

[39] Adams P D, Afonine P V, Bunkóczi G, et al. *PHENIX*: a comprehensive Python-based system for macromolecular structure solution. *Acta Crystallographica Section D: Structural Biology*, **2010**, *66*: 213–221.

[40] Mooers B H M, Brown M E. Templates for writing PyMOL scripts. *Protein Science*, **2021**, *30* (1): 262–269.

[41] Consortium T U. UniProt: the universal protein knowledgebase in 2023. *Nucleic Acids Research*, **2022**, *51* (D1): D523–D531.

[42] Tamura K, Stecher G, Kumar S. MEGA11: molecular evolutionary genetics analysis version 11. *Molecular Biology and Evolution*, **2021**, *38* (7): 3022–3027.

[43] Burley S K, Bhikadiya C, Bi C, et al. RCSB Protein Data Bank (RCSB.org): delivery of experimentally-determined PDB structures alongside one million computed structure models of proteins from artificial intelligence/machine learning. *Nucleic Acids Research*, **2023**, *51* (D1): D488–D508.

[44] Berman H M, Westbrook J, Feng Z, et al. The Protein Data Bank. *Nucleic Acids Research*, **2000**, *28* (1): 235–242.

[45] Varadi M, Anyango S, Deshpande M, et al. AlphaFold Protein Structure Database: massively expanding the structural coverage of protein-sequence space with high-accuracy models. *Nucleic Acids Research*, **2022**, *50* (D1): D439–D444.

[46] Gu Y, Zeng Y, Wang Z, et al. BamA β16C strand and periplasmic turns are critical for outer membrane protein insertion and assembly. *The Biochemical Journal*, **2017**, *474* (23): 3951–3961.

[47] Ni D C, Wang Y, Yang X, et al. Structural and functional analysis of the β-barrel domain of BamA from *Escherichia coli*. *FASEB Journal*, **2014**, *28* (6): 2677–2685.

[48] Noinaj N, Kuszak A J, Gumbart J C, et al. Structural insight into the biogenesis of β-barrel membrane proteins. *Nature*, **2013**, *501*: 385–390.

[49] Megrian D, Taib N, Witwinowski J, et al. One or two membranes? Diderm Firmicutes challenge the Gram-positive/Gram-negative divide. *Molecular Microbiology*, **2020**, *113* (3): 659–671.